Applied Thermal Engineering 280 (2025) 128271

Contents lists available at ScienceDirect

Applied Thermal Engineering

journal homepage: www.elsevier.com/locate/apthermeng

Research Paper

Thermal optimization of a PCM-based heat exchanger: A modeling approach

Giovanni Tanda *, Carlo Alberto Niccolini Marmont du Haut Champ, Stefano Barberis

DIME, Università degli Studi di Genova, via Montallegro 1, I-16145 Genova, Italy

ARTICLE INFO

Keywords:
Phase change material (PCM)
Energy storage
Heat exchanger
Vertical cavity
Lumped-parameter model

ABSTRACT

This study concerns the thermal performance of a thermal energy storage heat exchanger based on phase change materials (PCMs). The device consists of a series of vertical cavities filled with a PCM, which are subjected to heating and cooling along their vertical walls. A simplified theoretical model was developed using a lumped parameter approach and validated through experimental tests on a scaled-down cavity representative of the heat exchanger geometry. The primary objective of this study was to employ the modeling framework in formulating an optimization strategy aimed at improving system performance during the charging phase. Results indicate that enhancing the natural convection of the molten PCM, by integrating horizontal partitions within the cavity, substantially decreases the charging time, defined as the duration required for complete phase transition from solid to liquid. The reduction in charging time of a PCM-based heat exchanger prototype was found to be substantial (up to 50 %) when the effect of multiple partitions was investigated under constant wall temperature conditions, whereas the reduction was smaller (25–35 %) when heat exchange with an external fluid, at fixed mass flow rate and inlet temperature, was considered.

1. Introduction

Phase change materials (PCMs) are of particular interest due to their high latent heat storage capacity and their ability to maintain an isothermal behaviour during charging (melting) and discharging (solidification) processes. PCMs have been investigated across a broad spectrum of applications, including electronic equipment cooling [1,2], refrigeration [3], solar thermal and photovoltaic systems [4,5], ultrasonic thermal reactors [6], and spacecraft thermal management [7]. In particular, thermal energy storage using the latent heat provided by PCMs is an effective solution to increase the efficiency of energy systems in buildings [8–11]. A PCM-based heat exchanger stores excess thermal energy during off-peak periods, using either electricity (from photovoltaic panels or the grid) or hot water supplied by boilers, heat pumps, or district heating systems. This energy is used to charge the PCM, which melts and stores latent heat. When the building requires heating, the system switches to discharging mode, releasing the stored energy in a controlled and consistent manner. This approach reduces dependence on conventional energy-intensive heating and cooling systems during peak demand, thereby improving overall energy efficiency and lowering operational costs.

Numerical methods for PCM simulation during the charging process typically need to solve the governing equations, which involve complex factors such as the movement of the liquid–solid interface, the effect of temperature-dependent thermophysical properties, and the three-dimensional nature of the process. Due to these complexities, either large computing resources are required to provide accurate results, or simplified models that balance accuracy and computational efficiency, experimentally validated, are needed [12–15]. A simplified approach, based on a thermal network model combined with general relationships for natural convection heat transfer in the liquid phase, can be used to predict the dynamic thermal behavior of the heat exchanger, achieving a good compromise between computational efficiency and result accuracy [15]. In this regard, a lumped-parameter, one-dimensional model, supported by experiments performed on a scaled test section, has been developed to gain insight into the physical mechanisms governing PCM melting, with particular attention to strategies for enhancing the heat exchanger's performance, specifically by minimizing the charging time. The main novelty of this study lies in the development of a simple calculation tool, requiring minimal computational effort, and its application to a domain represented by a cavity heated from both vertical sides, which is a configuration not previously documented in the

* Corresponding author.
E-mail address: giovanni.tanda@unige.it (G. Tanda).

https://doi.org/10.1016/j.applthermaleng.2025.128271
Received 2 August 2025; Received in revised form 4 September 2025; Accepted 5 September 2025
Available online 7 September 2025

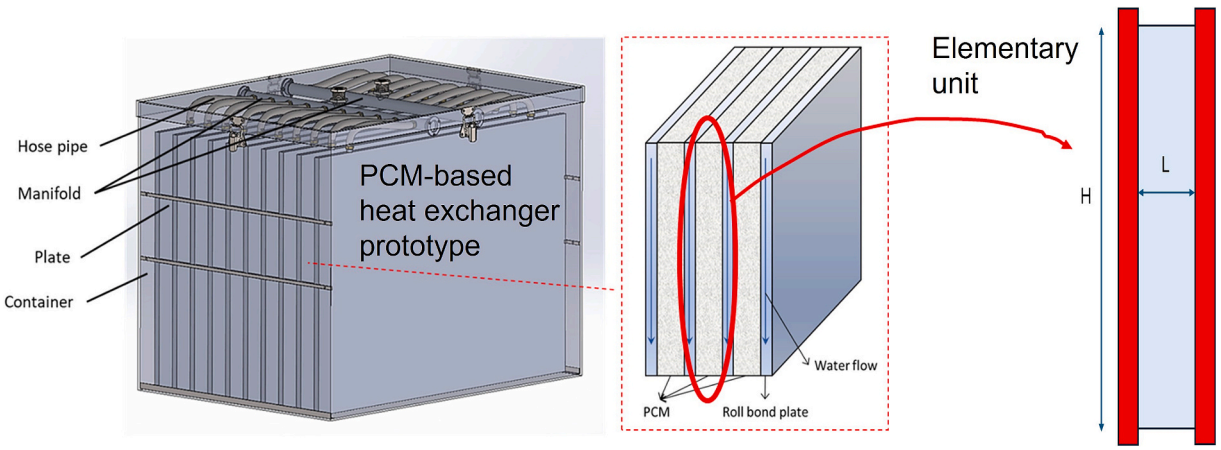

Fig. 1. Schematic of a PCM-based thermal energy storage heat exchanger. The elementary unit of the heat exchanger is shown on the right.

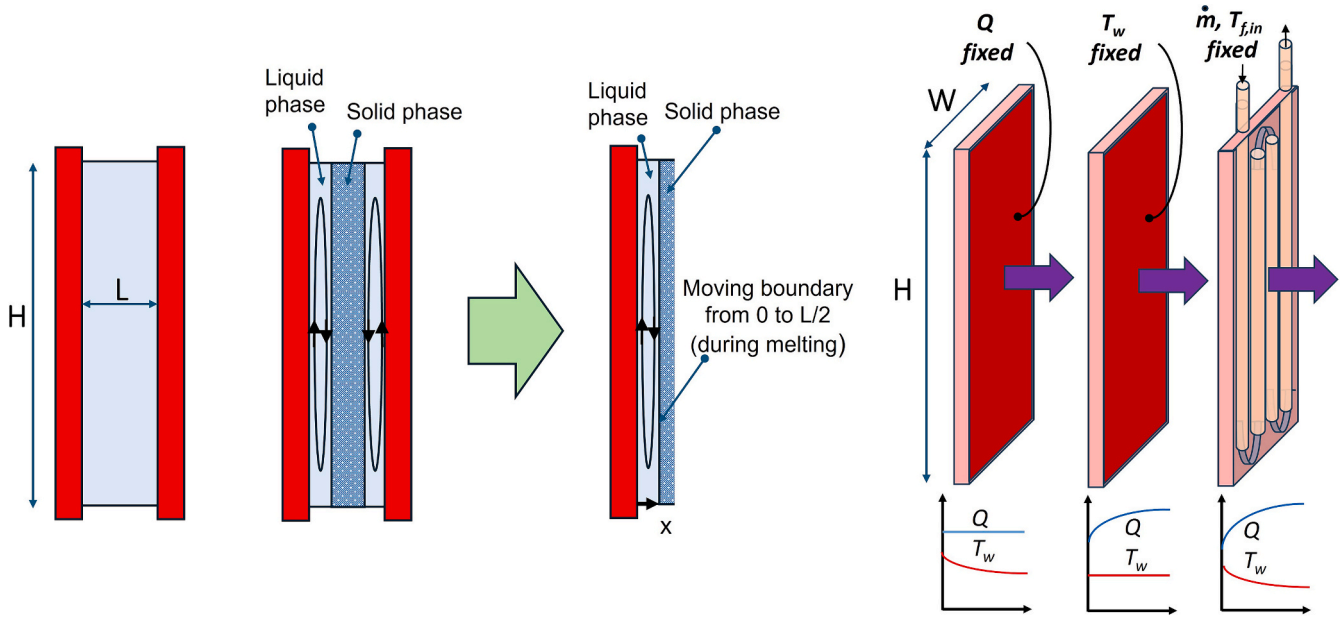

Fig. 2. The cavity heated from both vertical sides (left), the growing liquid layer due to the progressive melting of solid PCM (center), and the three thermal boundary conditions considered in the model (right).

literature, where cavities are typically heated from only one side.

2. Geometric and mathematical description

This study aims to optimize the operating conditions of a PCM-based heat exchanger designed to enhance energy savings in buildings. Fig. 1 presents a schematic of a heat exchanger prototype consisting of an array of parallel plates. Hot or cold water flows through internal channels within these plates, while the phase change material (PCM) is housed in the spaces between each adjacent pair of plates. This configuration enables efficient thermal exchange as the PCM undergoes phase transitions in response to the temperature of the circulating fluid. As shown in the figure, the basic unit of such a heat exchanger is represented by a two-dimensional cavity heated on both vertical sides, with the remaining walls unheated.

Achieving optimal performance from this system requires a comprehensive understanding of the physical processes governing PCM melting and solidification. In particular, design efforts must focus on minimizing the charging time, i.e., the duration needed for the complete melting of the PCM, since faster charging enhances the responsiveness and practicality of the system in real-world applications. Key factors influencing the charging time include heat transfer rates, natural convection within the molten PCM, and the geometric configuration of the heat exchanger.

Fig. 2 illustrates a vertical cavity with height H, width W, and depth L, bounded by two heated plates (whose temperature is indicated as T_w), and filled with PCM. This cavity constitutes a basic representation of the elementary unit of the heat exchanger shown in Fig. 1. The PCM is initially assumed to be in the solid phase at its melting temperature T_{ls}. When the wall temperature T_w exceeds the melting temperature T_{ls}, the PCM begins to melt, forming a thin layer of liquid, as shown in the figure. Initially, heat flows by thermal conduction, then the liquid starts to rise due to buoyancy forces, carrying heat upward while being cooled along the descending path near the liquid–solid interface. This recirculating flow promotes the progressive melting of the solid phase until the liquid layer reaches the midplane of the cavity, resulting in complete melting. This dynamic process can be modeled using an energy balance applied to half of the cavity, assuming symmetry. The energy balance states that the heat transfer rate through the developing liquid layer, originating from the heated wall with an area of $H \times W$, corresponds to

Table 1
Literature correlations for Nu_H (=$h\,H/k_l$) in a vertical cavity heated on one side [16–18] as a function of the Rayleigh number $Ra_H = \beta g(T_w\text{-}T_{ls})H^3Pr/\nu^2$, the Prandtl number $Pr = \nu\rho_l\,c_l/k_l$ and the aspect ratio H/x. Some correlations have been rearranged to account for the different characteristic length used in the refs. and here.

Correlation for Nu_H	Code (Fig. 3)	Validity range
$0.18\,(Pr_mRa_H)^{0.29}(H/x)^{0.13}$ [17]; Pr_m=$Pr/(0.2+Pr)$	a	$1 < H/x < 2$
$0.22\,(Pr_mRa_H)^{0.28}(H/x)^{-0.09}$ [17]; Pr_m=$Pr/(0.2+Pr)$	b	$2 < H/x < 10$
$0.42(Pr_m)^{0.012}(Ra_H)^{0.25}(H/x)^{-0.05}$ [18]; constant-heat flux	c	$10 < H/x < 40$
$0.25\,(Ra_H)^{0.25}$ [18]; isothermal walls	d	n.a.
$0.364\,(Ra_H)^{0.25}$ [16];	e	$H/x > 1$
H/x; pure conduction limit (i.e., $Nu_H(x/H) = 1$)	f	$H/x \to \infty$

the enthalpy change over time of the solid phase.

Introducing the latent heat of fusion h_{ls}, the density of the solid phase ρ_s, and the Nusselt number $Nu_H = q\,H/[k_l\,(T_w - T_{ls})]$, where q is the heat flux through the liquid, $(T_w - T_{ls})$ is the temperature difference across the liquid layer, and k_l is the thermal conductivity of the liquid phase, it follows that

$$Nu_H k_l (T_w - T_{ls})/H = h_{ls}\rho_s dx/dt \tag{1}$$

where x denotes the thickness of the liquid phase, which ranges from zero to half the depth of the cavity (due to the symmetry of the phenomenon), and t is the time. The Nusselt number is taken from established correlations in the literature for natural convection heat transfer in vertical cavities heated from the sides. It typically depends on the PCM properties, the wall-to-solid temperature difference, and the aspect ratio of the region where the liquid phase recirculates (i.e., the ratio of the height H to the liquid layer thickness x), which evolves over time.

The solution of Eq. (1) describes the time evolution of the liquid–solid interface during the melting process, subject to the following assumptions: (i) the interface moves only in the x-direction (i.e., the phenomenon is one-dimensional, and all variables depend solely on x), (ii) the heat storage in the liquid phase is neglected, (iii) PCM is initially in the solid state at its melting temperature (i.e., not subcooled, as in real applications), and (iv) the thermophysical properties of both the liquid and solid phases are constant.

The search for the function $x(t)$ can be carried out under three different thermal boundary conditions, illustrated on the right-hand side of Fig. 2:

1) **Constant heat transfer rate**. A constant heat transfer rate $Q = q \times H \times W$ (or heat flux q) is supplied to PCM. In this case, the wall temperature T_w varies during the transient process, as the Nusselt number is continuously adjusted based on the evolving aspect ratio H/x of the liquid layer.
2) **Constant wall temperature**. A fixed wall temperature T_w is maintained. Consequently, the heat transfer rate Q (and the heat flux q) varies over time during the transient melting process.
3) **Convective heat exchange with external fluid.** Heat is transferred to the PCM from a hot external fluid circulating through a tube (with an assigned hydraulic diameter D) embedded within the heated plate. The fluid enters at a constant inlet temperature $T_{f,in}$ and flows at a constant mass flow rate $\dot{m}$. Under this last thermal boundary condition, two additional energy balance equations can be formulated. The first expresses the balance between the enthalpy change of the external fluid and the heat transfer rate from the heated wall to the PCM:

$$\frac{1}{2}\dot{m}c_{p,f}\left(T_{f,in} - T_{f,out}\right) = WNu_H k_l\left(T_w - T_{ls}\right) \tag{2}$$

where $c_{p,f}$ is the specific heat of the external fluid, and $T_{f,out}$ is its outlet temperature. The factor $^1/_2$ accounts for the fact that the model considers only half of the cavity.

The second additional equation represents the balance between the heat transfer rate from the external fluid to the wall and the enthalpy change of the external fluid:

$$h_f WH\left(T_{f,avg} - T_w\right) = \frac{1}{2}\dot{m}c_{p,f}\left(T_{f,in} - T_{f,out}\right) \tag{3}$$

where the heat transfer area between the external fluid and the plate is approximated as $W \times H$, $T_{f,avg} = (T_{f,in} + T_{f,out})/2$, and the thermal resistance of the plate material is neglected. To evaluate the heat transfer coefficient h_f inside the duct, an appropriate correlation must be selected, such as the one for fully developed laminar flow or the Dittus-Boelter equation for turbulent flow [16]. At each time instant, the three unknowns T_w, $T_{f,out}$, and x are obtained by solving the coupled system of Eqs. (1)-(3). It is evident that this thermal boundary condition leads to time-dependent variations in both the heat transfer rate Q and the wall temperature T_w.

Literature correlations for Nu_H, taken from [16–18] and summarized in Table 1, are graphically illustrated in Fig. 3. The figure specifically refers to a relatively high Prandtl number (as typically encountered in PCMs) and to $Ra_H = 10^8$; however, similar trends are observed for Ra_H values ranging from 10^6 to 10^{10}. As the aspect ratio of the liquid region, H/x, increases, the efficiency of free-convective heat transfer through the liquid decreases, gradually approaching the pure conduction limit for very large H/x values. Based on an analysis of the available relationships, correlation (b), valid for H/x in the range of 2 to 10, has been adopted in the present work. If necessary, it has been extrapolated beyond its original range of validity. For very large H/x values, where correlation (b) yields $Nu_H(x/H) < 1$, the value of $Nu_H(x/H)$ was set to 1, corresponding to the pure conduction limit. Conversely, when very small values *of* H/x arise as a result of the increasing liquid layer thickness, correlation (b) was employed up to its intersection with correlation (a), which typically occurs for H/x between 1 and 1.35, depending on Ra_H and Pr. For H/x below this threshold, a condition rarely encountered in PCM-based heat exchangers, Eq. (b) was replaced by Eq. (a) to capture the inverted trend of the Nu vs. H/x relationship as H/x approaches very small values.

When the cavity filled with PCM is tall and slender, as in the case of the envisioned heat exchanger prototype, the developing liquid layer is confined within a narrow gap, resulting in a high aspect ratio. As illustrated in Fig. 3, this geometry limits the effectiveness of buoyancy-driven convection, often leading to low heat transfer coefficients or even purely conductive heat transfer across the essentially stagnant liquid layer. To enhance heat transfer performance under these conditions, one potential strategy is the insertion of multiple fins or partitions within the cavity, a practice that has been successfully documented in [19–24]. For instance, horizontal regularly spaced partitions divide the cavity into smaller subcavities with lower aspect ratios, thereby promoting recirculation of the molten PCM, as shown in the top-right corner of Fig. 4. In addition to enhancing convective motion, the presence of thin metallic partitions increases the effective heat transfer area through the fin effect, though this contribution is not accounted for in the present model. Adapting the model to this modified geometry requires redefining the characteristic length used in the Rayleigh and Nusselt number calculations. Specifically, the height of each subcavity, denoted as H' and given by H divided by the number of subcavities, replaces the original cavity height H in the definitions of both Rayleigh and Nusselt numbers, as well as in the updated aspect ratio H'/x of the liquid layer.

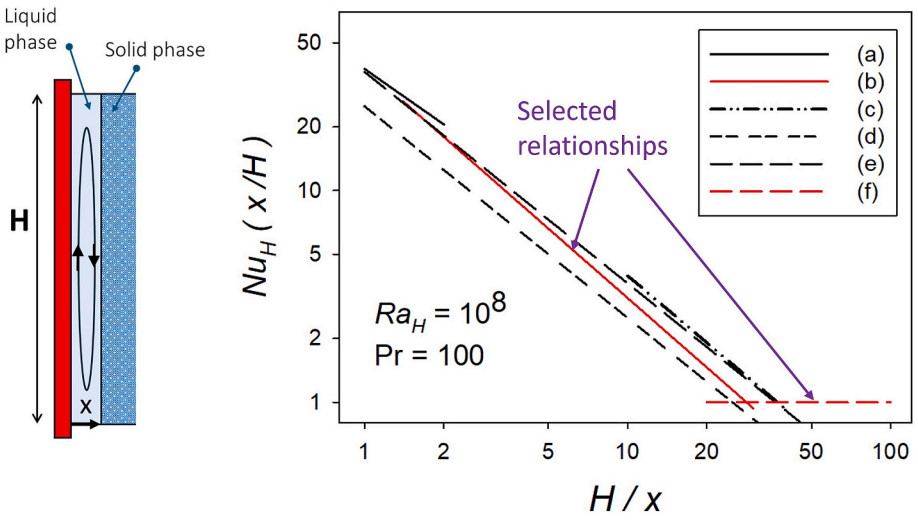

Fig. 3. Plot of $Nu_H(x/H)$ versus aspect ratio H/x based on the literature correlations from Table 1, for $Ra_H = 10^8$ and $Pr = 100$. Similar trends are observed for Ra_H values within the range of interest (10^6 – 10^{10}).

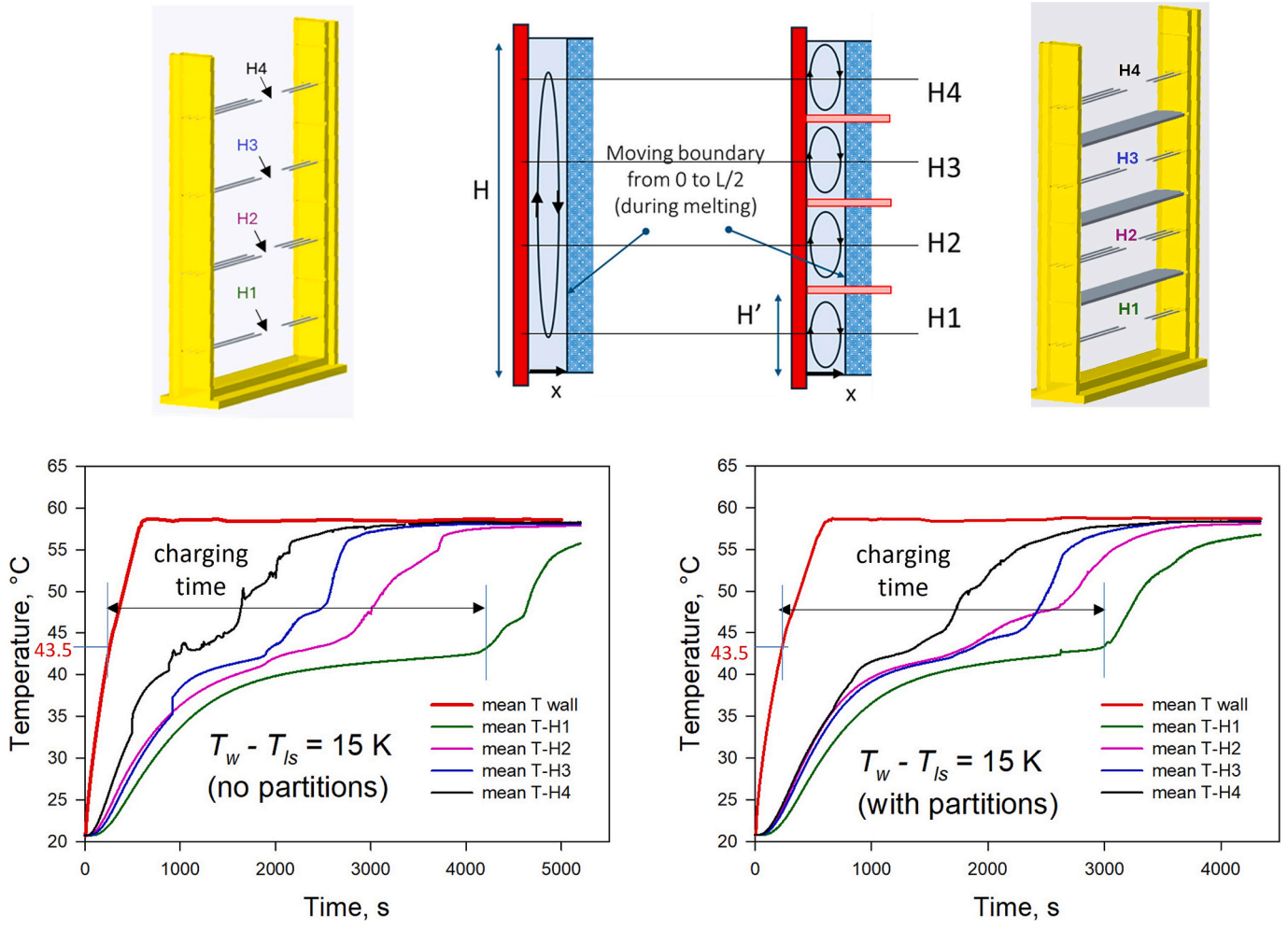

Fig. 4. Measured wall and PCM (lauric acid) temperatures, averaged over four horizontal planes (H1, H2, H3, and H4) where thermocouples are installed (individual locations shown in the 3D sketches). Experimental charging times are also indicated.

3. Model validation

The results provided by the model were compared with experimental data obtained for a cavity filled with lauric acid as PCM, whose properties are listed in Table 2 [25]. The cavity (100 mm high, 68 mm wide, and 30 mm deep) was electrically heated on both vertical sides, each with a heat transfer area of 100 × 68 mm^2. Plane heaters were glued to 8 mm-thick aluminum plates, whose high thermal conductivity

Table 2
Properties of lauric acid [25].

Melting temperature T_{ls}	43.5 °C
Latent heat of fusion h_{ls}	187.2 kJ/kg
Density of liquid/solid ρ_l/ρ_s	885/940 kg/m^3
Thermal conductivity of liquid/solid k_l/k_s	0.14/0.16 W/m K
Specific heat of liquid/solid c_l/c_s	2.39/2.18 kJ/kg K
Kinematic viscosity ν	6.7×10^{-6} m^2/s
Thermal expansion coefficient β	0.0008 K^{-1}
Prandtl number Pr	101

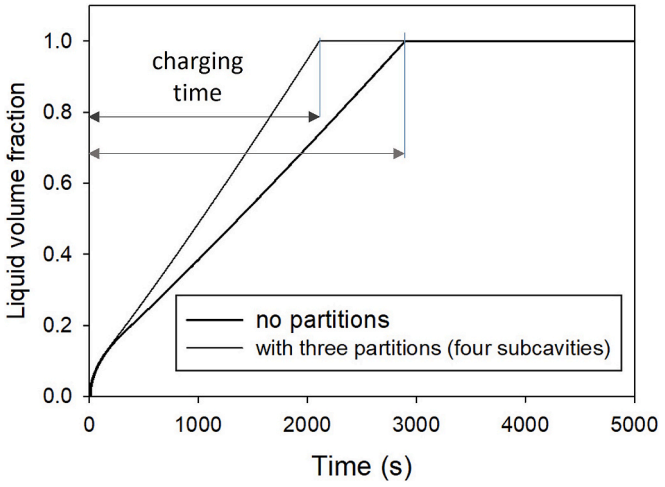

Fig. 5. Calculated liquid volume fraction during the melting process of lauric acid (PCM) for the experimentally tested cavity. Corresponding charging times are also indicated.

ensured a fairly uniform temperature at any given time. Two experiments were conducted: one without partitions and another with three partitions dividing the cavity into four subcavities. In both cases, an adjustable input power was applied to maintain a constant wall-to-melting temperature difference of 15 K (i.e., T_w = 58.5 °C, T_{ls} = 43.5 °C), except during a brief initial transient. Both the heated side walls and the PCM were instrumented with numerous sheathed thermocouples to monitor local and average temperature variations during the melting process. Thermocouples with a diameter of 0.5 mm were used within the heated plates, while 0.25-mm diameter thermocouples were placed in the PCM, as shown in the 3D sketches of Fig. 4.

The plots in Fig. 4 show the measured temporal evolution of PCM temperature, averaged over four different horizontal planes. They also indicate the time required for the complete melting of the PCM (referred to as the "charging time"), which begins when the wall temperature reaches the melting temperature T_{ls} and ends when all thermocouples display a clear rise above T_{ls}. In the case without partitions, a consistent time delay in local PCM melting is observed as the elevation decreases. This phenomenon challenges the assumption of a one-dimensional growth (along the horizontal coordinate) of the liquid layer, since melting is also affected by the vertical coordinate, and it highlights the inefficiency of natural convection in the liquid layer due to the relatively large aspect ratio. In contrast, the case with partitions exhibits a reduced elevation-dependent melting delay. The introduction of partitions reduced the measured charging time from 4000 to 2770 s, corresponding to a 30.8 % decrease.

Fig. 5 shows the liquid volume fraction predicted by the model for both configurations, obtained by solving Eq. (1) under the constant wall temperature boundary condition and using a time step of 1 s. A smaller time step (for instance, 0.1 s) results in numerical errors in the charging time of less than 0.2 %. The calculated charging times are 2898 s without partitions and 2111 s with three partitions (as in the experiments). The predicted time for the complete melting of the PCM is approximately 25 % shorter than the experimental value. This discrepancy can be attributed to some of the model's limiting assumptions (e.g., the PCM being initially at the melting temperature rather than at ambient temperature as in the experiments, the neglect of heat storage in the liquid phase, and uncertainties in the thermophysical properties). Nevertheless, the model predicts a 27.2 % reduction in charging time due to the presence of partitions, which agrees reasonably well with the 30.8 % reduction observed experimentally. The slight discrepancy (of about 12 %) may also be due to the fin effect present in the experiments but not considered in the model, which likely contributes to further accelerating the melting process in the partitioned configuration.

A further comparison was made with experimental data from [19,23], obtained for lauric acid and n-octadecane in the presence of one or three horizontal fins/partitions. Experiments in [19] were conducted at constant wall temperatures (three different levels), whereas in [23] the mean wall temperatures for the unpartitioned and partitioned cavities differed (as the two configurations were heated supplying the same heat transfer rate); the respective reported wall temperatures were therefore used in the model. The reduction in charging time experimentally observed in [19] (T_w in the 55–70 °C range, T_{ls} = 43.5 °C) was 17–19 % with one horizontal fin and 36–38 % with three horizontal fins. Calculations predicted a 16 % reduction with a single partition and 26 % with three partitions. Experiments reported in [23] (T_w = 47 °C without partitions and 44 °C with partitions, T_{ls} = 28 °C) showed a 15 %

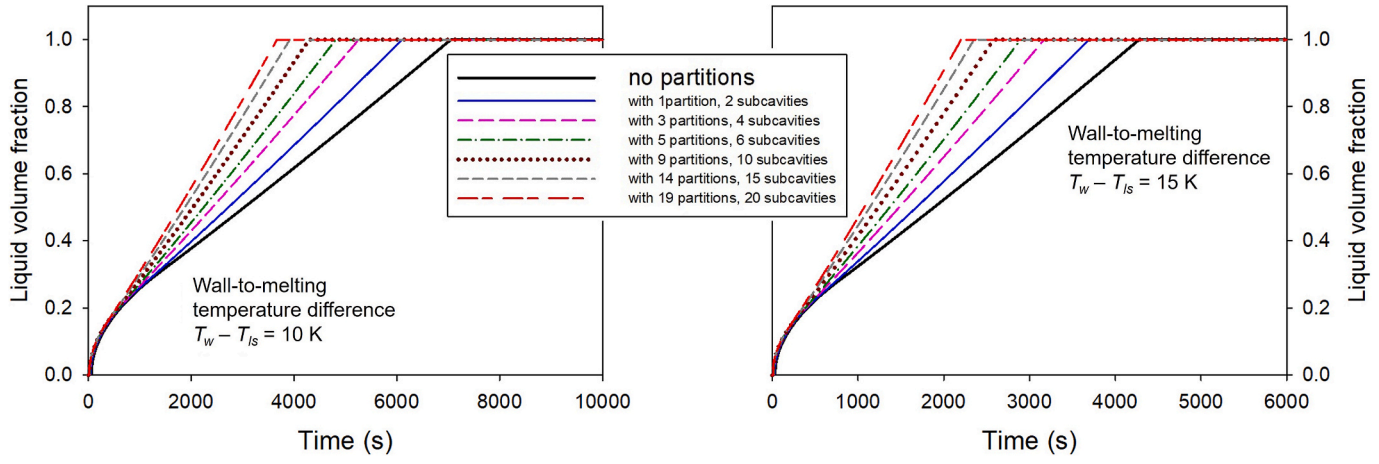

Fig. 6. Liquid volume fraction over time for configurations without and with partitions, under constant wall temperature conditions at two different temperature levels.

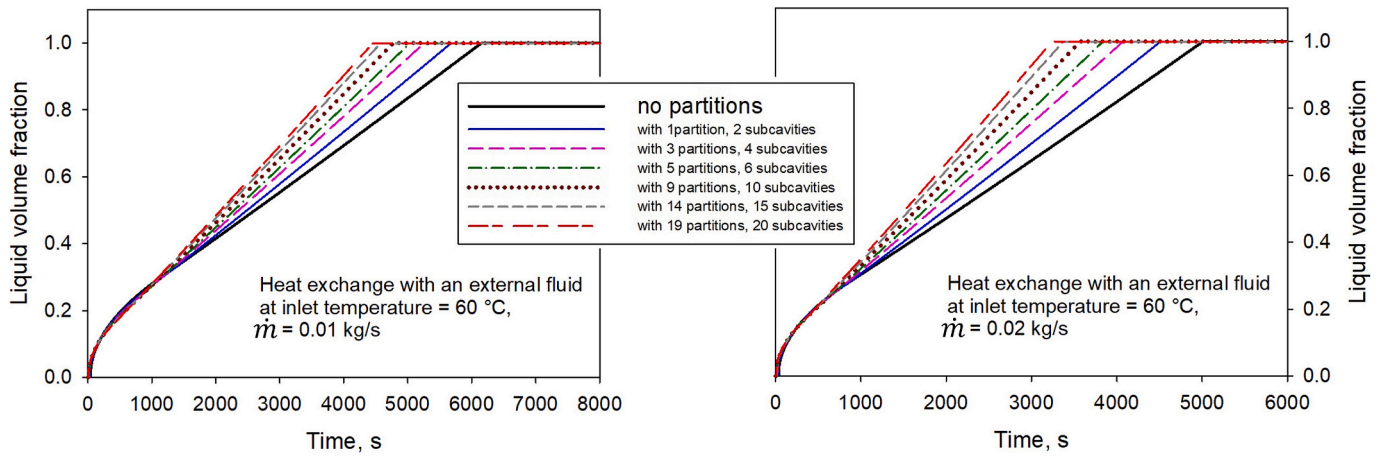

Fig. 7. Liquid volume fraction over time for configurations without and with partitions, under heat exchange with an external fluid at a fixed inlet temperature and two different mass flow rates.

reduction in charging time with three partitions, compared to a 10 % reduction predicted by the model. Considering the relative simplicity of the one-dimensional model and the different operating conditions assumed in [19,23] (for instance, heating applied only to one side of the cavity, tests starting from ambient temperature rather than the melting temperature, and the fin effect neglected in the model), the agreement between model results and literature data can be considered satisfactory.

4. Results and discussion

Once the reliability of the model had been validated, calculations were conducted using a cavity that replicates the dimensions of the heat exchanger prototype, specifically, a series of vertical cavities measuring 0.6 m in height, 1.0 m in width, and 0.03 m in depth (distance between the heated plates). Lauric acid (properties listed in Table 2) was used as PCM. The calculations were performed with a time step ranging from 0.2 to 1 s, depending on the input parameters and boundary conditions, while maintaining the numerical error below 0.2 %. The objective of the calculations was to evaluate whether the introduction of a number of equally spaced horizontal partitions could effectively reduce the charging time of the PCM-filled cavity, which represents the elementary unit of the heat exchanger.

As previously noted, three different heating conditions can be applied to the vertical walls of the cavity. When the same heat transfer rate is applied in both the partitioned and non-partitioned configurations, the wall temperature is lower in the partitioned case; however, the charging time remains unchanged. Therefore, this condition is not relevant for the intended application. Conversely, assuming the same wall temperature in both cases leads to higher heat transfer rates in the partitioned configuration. This is attributed to a more favorable aspect ratio of the liquid region, which, under the same driving potential (i.e., same wall-to-melting temperature difference), enhances buoyancy-driven recirculation and thus improves natural convective heat transfer. As a result, the time required for complete melting of the PCM is reduced. Results for the constant-wall-temperature condition are shown in Fig. 6 for two values of $T_w - T_{ls}$, namely 10 and 15 K. Inspection of the figure reveals that, for these temperature differences, a noticeable reduction in charging time is achieved even with a small number of partitions (e.g., one or three).

A further comparison was carried out under a different constraint, whereby the same mass flow rate $\dot{m}$ of an external fluid at a specified inlet temperature $T_{f,in}$ was imposed. Two values of the mass flow rate ($\dot{m}$ = 0.01 and 0.02 kg/s) were considered. The hydraulic diameter of the tube embedded in the heated plate was assumed to be D = 0.005 m, corresponding to a Reynolds number, for the external fluid flowing inside the tube, greater than 5000. Under these conditions, the flow was considered turbulent, and the heat transfer coefficient inside the tube was calculated using the Dittus-Boelter correlation [16]. Fig. 7 presents the results in terms of liquid volume fraction versus time: the inclusion of partitions continues to yield a reduction in charging time, exhibiting similar behavior to that observed under the constant wall temperature condition.

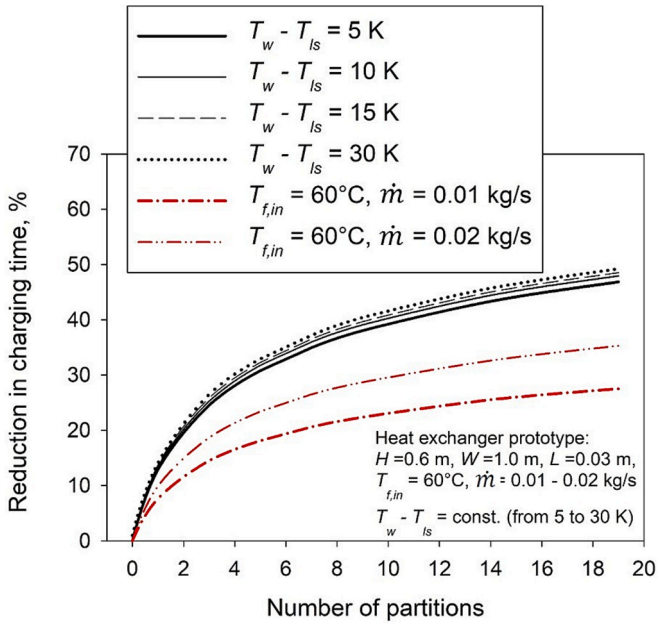

Fig. 8. Percentage reduction in PCM charging time resulting from the introduction of horizontal partitions, evaluated under two thermal boundary conditions: constant wall temperature, and heat exchange with an external fluid circulating at fixed mass flow rate and inlet temperature.

The percentage reduction in the PCM charging time for each module of the heat exchanger prototype is illustrated in Fig. 8. For both thermal boundary conditions, either a fixed wall temperature or heat exchange with an external fluid at constant mass flow rate and inlet temperature, the presence of horizontal partitions consistently reduces the charging time; however, a saturation effect is observed. Indeed, as the number of partitions increases substantially, the reduction in charging time becomes less significant, as also reported in [22].

Specifically, when a constant wall temperature is imposed and kept equal in both the partitioned and unpartitioned configurations, charging

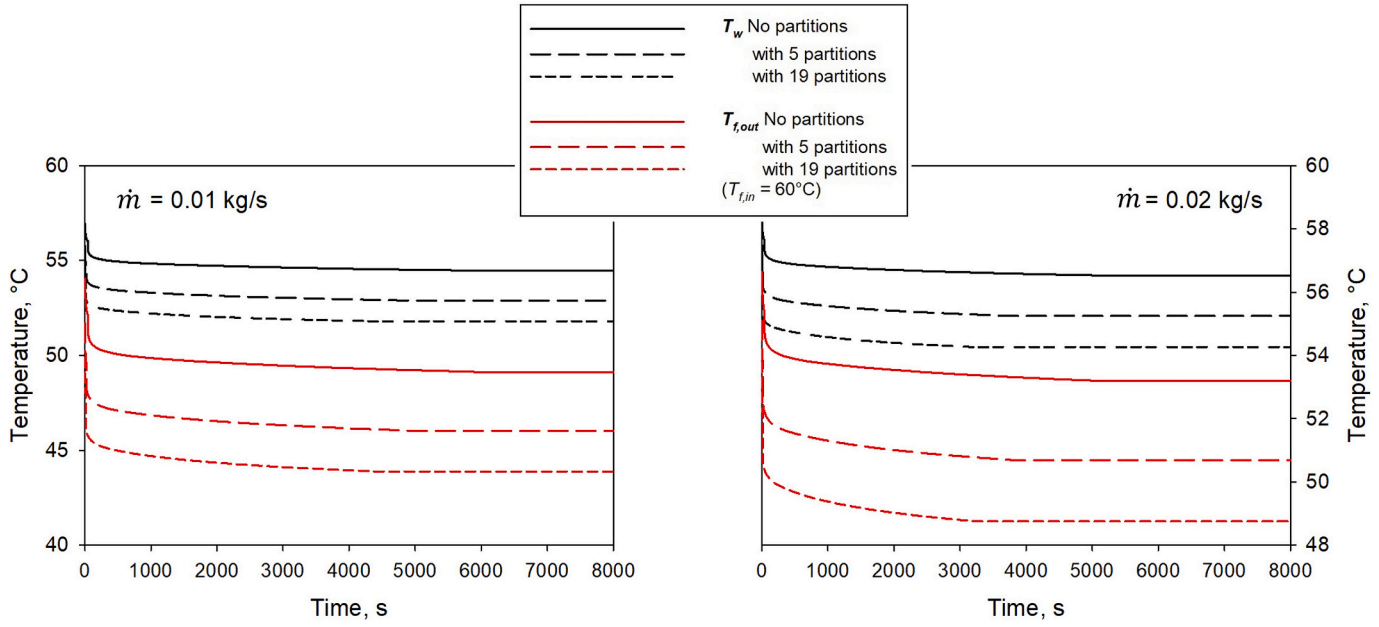

Fig. 9. Wall temperature and outlet fluid temperature for configurations without partitions and with 5 or 19 partitions, at two different mass flow rates.

times are reduced by up to 50 %, with negligible influence from the wall-to-melting temperature difference within the 5–30 K range. In contrast, when heat is supplied via internal circulation of a hot external fluid, a condition more representative of real operating scenarios, the maximum reduction in charging time due to partitions is approximately 25–35 %, depending on the mass flow rate (0.01 to 0.02 kg/s), with greater reductions corresponding to higher mass flow rates. This comparatively less favorable outcome under external fluid circulation is further elucidated in Fig. 9, which displays wall and outlet fluid temperatures for cases without partitions and with 5 or 19 partitions. The inlet temperature is fixed at 60 °C, and two mass flow rates (0.01 and 0.02 kg/s) are considered. Under these conditions, where the wall temperature decreases over time, two opposing effects can be observed. On the one hand, the presence of partitions reduces the wall-to-melting temperature difference compared to the unpartitioned case, which tends to limit the potential benefits of the partitions. On the other hand, partitions significantly increase the inlet-to-outlet temperature difference of the external fluid, resulting in a much higher heat transfer rate from the fluid to the PCM despite the reduced wall-to-melting temperature difference. Consequently, partitions still lead to a marked reduction in charging time, although the improvement is less pronounced than in the case of a fixed wall temperature. It is also worth noting that, in principle, the two scenarios converge when a sufficiently high mass flow rate is imposed, such that the wall temperature remains nearly constant and closely follows the inlet temperature throughout the charging process.

5. Conclusions

In this study, the melting process within a vertical cavity, representing the elementary unit of a PCM-based thermal energy storage heat exchanger, was modeled using a simplified one-dimensional approach. The model relies on an energy balance that incorporates standard heat transfer coefficient correlations for natural convection in the forming liquid layer, under different thermal boundary conditions at the wall-PCM interface. Validation was performed against experimental data obtained from a scaled-down cavity as well as data reported in the literature.

The main objective was to identify an optimized cavity configuration, filled with lauric acid at its melting temperature, that could significantly reduce the charging time. This was achieved by introducing a set of equally spaced horizontal partitions dividing the cavity into smaller subcavities. The partitions were designed to enhance natural convection in the liquid phase by providing a more favorable aspect ratio for each liquid region.

From the perspective of the heat exchanger design, the model calculations showed that the introduction of partitions led to a substantial decrease in charging time, up to 50 % for the considered input parameters, under idealized conditions of constant wall temperature. Under more realistic operating conditions, where heat is supplied by an external fluid at a fixed mass flow rate and inlet temperature, the reduction in charging time was more moderate, reaching approximately 25–35 % at most.

CRediT authorship contribution statement

Giovanni Tanda: Writing – review & editing, Writing – original draft, Validation, Software, Methodology, Investigation, Formal analysis, Data curation, Conceptualization. **Carlo Alberto Niccolini Marmont du Haut Champ:** Writing – review & editing, Investigation, Formal analysis, Data curation. **Stefano Barberis:** Writing – review & editing, Project administration, Investigation, Funding acquisition, Conceptualization.

Declaration of competing interest

The authors declare that they have no known competing financial interests or personal relationships that could have appeared to influence the work reported in this paper.

Acknowledgements

This work was supported by the European Union's Horizon Europe Framework Program for Research and Innovation (THUMBS UP project) under grant agreement No. 1010969291.

Data availability

Data will be made available on request.

References

[1] R. Kandasamy, X.Q. Wang, Application of phase change materials in thermal management of electronics, Appl. Therm. Eng. 27 (2007) 2822–2832, https://doi.org/10.1016/j.applthermaleng.2006.12.013.

[2] R. Baby, C. Balaji, Experimental investigations on phase change material based finned heat sinks for electronic equipment cooling, Int. J. Heat Mass Transf. 55 (2012) 1642–1649, https://doi.org/10.1016/j.ijheatmasstransfer.2011.11.020.

[3] M.M. Joybari, F. Haghighat, J. Moffat, P. Sra, Heat and cold storage using phase change materials in domestic refrigeration systems: The state-of-the-art review, Energ. Buildings 106 (2015) 111–124, https://doi.org/10.1016/j.enbuild.2015.06.016.

[4] V. Goel, A. Saxena, M. Kumar, A. Thakur, A. Sharma, V. Bianco, Potential of phase change materials and their effective use in solar thermal applications: A critical review, Appl. Therm. Eng. 219 (2023) 119417, https://doi.org/10.1016/j.applthermaleng.2022.119417.

[5] S.S. Chandel, T. Agarwal, Review of cooling techniques using phase change materials for enhancing efficiency of photovoltaic power systems, Renew. Sustain. Energy Rev. 73 (2017) 1342–1351, https://doi.org/10.1016/j.rser.2017.02.001.

[6] A. Chibani, A. Dehane, S. Merouani, O. Hamdaoui, Phase Change Material (PCM)-based thermal storage system for managing the sonochemical reactor heat: Thermodynamic analysis of the liquid height impact, Ultrason. Sonochem. 98 (2023) 106483, https://doi.org/10.1016/j.ultsonch.2023.106483.

[7] J. Khan, P. Singh, Review on phase change materials for spacecraft avionics thermal management, J. Storage Mater. 87 (2024) 111369, https://doi.org/10.1016/j.est.2024.111369.

[8] A. Waqas, Z.U. Din, Phase change material (PCM) storage for free cooling of buildings—A review, Renew. Sustain. Energy Rev. 18 (2013) 607–625, https://doi.org/10.1016/j.rser.2012.10.034.

[9] R. Stropnik, R. Koželj, E. Zavrl, U. Stritih, Improved thermal energy storage for nearly zero energy buildings with PCM integration, Sol. Energy 190 (2019) 420–426, https://doi.org/10.1016/j.solener.2019.08.041.

[10] P.K.S. Rathore, S.K. Shukla, Potential of macroencapsulated PCM for thermal energy storage in buildings: A comprehensive review, Constr. Build. Mater. 225 (2019) 723–744, https://doi.org/10.1016/j.conbuildmat.2019.07.221.

[11] P.K.S. Rathore, S.K. Shukla, Enhanced thermophysical properties of organic PCM through shape stabilization for thermal energy storage in buildings: A state of the art review, Energ. Buildings 236 (2021) 110799, https://doi.org/10.1016/j.enbuild.2021.110799.

[12] C. Yao, X. Kong, Y. Li, Y. Du, C. Qi, Numerical and experimental research of cold storage for a novel expanded perlite-based shape-stabilized phase change material wallboard used in building, Energ. Conver. Manage. 155 (2018) 20–31, https://doi.org/10.1016/j.enconman.2017.10.052.

[13] M. Mozafari, A. Lee, J. Mohammadpour, Thermal management of single and multiple PCMs based heat sinks for electronics cooling, Therm. Sci. Eng. Prog. 23 (2021) 100919, https://doi.org/10.1016/j.tsep.2021.100919.

[14] Y. Huang, X. Liu, Charging and discharging enhancement of a vertical latent heat storage unit by fractal tree-shaped fins, Renew. Energy 174 (2021) 199–217, https://doi.org/10.1016/j.renene.2021.04.066.

[15] J. Yin, S. Wang, X. Hou, Z. Wang, M. Ye, Y. Xing, Transient prediction model of finned tube energy storage system based on thermal network, Appl. Energy 336 (2023) 120861, https://doi.org/10.1016/j.apenergy.2023.120861.

[16] A. Bejan, Convection Heat Transfer, fourth ed., Wiley, 2013.

[17] I. Catton, Natural convection in enclosures, in: Proceedings of the 6th Int. Heat Transfer Conf., Toronto, Canada (1978), Vol.6, pp.13−31.

[18] R.K. MacGregor, A.F. Emery, Free convection through vertical plane layers − Moderate and high Prandtl number fluids, ASME Journal of Heat Transfer 91 (1969) 391–401, https://doi.org/10.1115/1.3580194.

[19] B. Kamkari, H. Shokouhmand, Experimental investigation of phase change material melting in rectangular enclosures with horizontal partial fins, Int. J. Heat Mass Transf. 78 (2014) 839–851, https://doi.org/10.1016/j.ijheatmasstransfer.2014.07.056.

[20] N. Soares, A.R. Gaspar, P. Santos, J.J. Costa, Experimental study of the heat transfer through a vertical stack of rectangular cavities filled with phase change materials, Appl. Energy 142 (2015) 192–205, https://doi.org/10.1016/j.apenergy.2014.12.034.

[21] N.I. Ibrahim, F.A. Al-Sulaiman, S. Rahman, B.S. Yilbas, A.Z. Sahin, Heat transfer enhancement of phase change materials for thermal energy storage applications: A critical review, Renew. Sustain. Energy Rev. 74 (2017) 26–50, https://doi.org/10.1016/j.rser.2017.01.169.

[22] M.S. Mahdi, H.B. Mahood, A.N. Campbell, A.A. Khadom, Natural convection improvement of PCM melting in partition latent heat energy storage: Numerical study with experimental validation, Int. Commun. Heat Mass Transfer 126 (2021) 105463, https://doi.org/10.1016/j.icheatmasstransfer.2021.105463.

[23] Y.Y. Ji, D.K. Sohn, H.S. Ko, The effect of baffles on vertical wall PCM to enhance natural convection, Int. J. Heat Mass Transf. 222 (2024) 125187, https://doi.org/10.1016/j.ijheatmasstransfer.2024.125187.

[24] F.L. Rashid, N.S. Dhaidan, A.J. Mahdi, S.A. Kadhim, K.A. Hammoodi, M.A. Al-Obaidi, H.I. Mohammed, S. Ahmad, S. Salahshour, E.B. Agyekum, Heat transfer enhancement of phase change materials using tree shaped fins: A comprehensive review, Int. Commun. Heat Mass Transfer 162 (2025) 108573, https://doi.org/10.1016/j.icheatmasstransfer.2024.108573.

[25] C. J. Troxler, T. B. Freeman, R. M. Rodriguez, S. K. S. Boetcher, Experimental and numerical investigation of lauric acid melting at suboptimal inclines, ASME Open Journal of Engineering 2 (2023) 021011-1. https://doi.org/10.1115/1.4056348.